

# Antibody Clicking as a Strategy to Modify Antibody Functionalities on the Surface of Targeted Cells

Toru Komatsu,\* Etsu Kyo, Haruki Ishii, Kyoji Tsuchikama, Aiko Yamaguchi, Tasuku Ueno, Kenjiro Hanaoka, and Yasuteru Urano\*



Cite This: <https://dx.doi.org/10.1021/jacs.0c05331>



Read Online

ACCESS |



Metrics & More



Article Recommendations



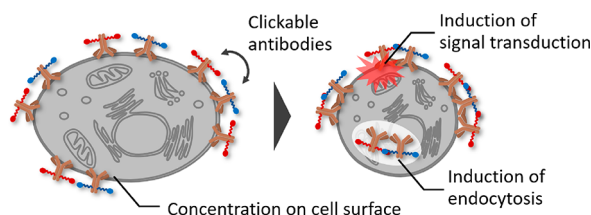
Supporting Information

**ABSTRACT:** We established a methodology for initiating cross-linking of antibodies selectively on the cell surface through intermolecular copper-free click reactions facilitated by increased effective concentrations of antibodies binding to target antigens. Upon cross-linking of tetrazine- and bicyclononyne-modified trastuzumab on the surface of HER2-overexpressing cells, increased antibody uptake and activation of intracellular signaling were observed. Our findings demonstrate that the cross-linking reaction can significantly alter the biophysical properties of proteins, activating their unique functionalities on targeted cells to realize an increased cargo delivery and synthetic manipulation of cellular signaling.

Antibodies are molecules that bind to antigens with high specificity and affinity and are widely used in biological studies and for therapeutic purposes.<sup>1</sup> Recently, researchers have tried to expand the functions of antibody using protein engineering<sup>2,3</sup> and chemical modifications.<sup>4–9</sup> Modifications of antibodies using chemical tools are mainly performed to add unique functionality, such as cytotoxicity, or molecular imaging capacity. In general, modifications are not designed for altering the nature of the antibody as a carrier, and few studies have reported molecular designs that aim to alter the physical properties of antibodies to confer desired functionality.

Recent studies have reported that, in photoimmunotherapy, the increased hydrophobicity of antibodies upon photoirradiation causes cytotoxicity of the conjugates, due to the formation of protein aggregates.<sup>6,7</sup> This indicates that the alteration of the physical properties of antibodies (e.g., tendency to aggregate) can be a basis for eliciting unique functionality (e.g., cytotoxicity). In this study, we developed a methodology for inducing antibody aggregation using chemical reactions that spontaneously occur on the cell surface without photoirradiation, leading to altered behaviors and functionalities of antibodies. We envisaged that the increased effective concentration of antibodies binding to densely expressed target antigens could be utilized to facilitate selective cross-linking on the cell surface (Scheme 1).

## Scheme 1. Design of Cell Surface Antibody Cross-Linking



Copper-free click reactions, which include inverse-electron-demand Diels–Alder reactions, are useful bioorthogonal reactions that enable the selective and rapid formation of covalent bonds between molecules.<sup>10–12</sup> These reactions show high regioselectivity, and we expected that antibody pairs labeled with appropriate pairs of clickable linkers should form cross-linked products when they are close to each other. We prepared a set of antibody-clicking molecules, collectively termed antibody clickers (AbCs), consisting of tetrazine (Tz)/methyltetrazine (MTz) and bicyclononyne (BCN) attached with a protein labeling site (*N*-hydroxysuccinimidyl ester) via varied lengths of polyethylene glycol (PEG) linkers (Figure 1a, Scheme S1). We hypothesized that linkers of sufficient length are desirable for proper interactions within AbCs upon antibody binding to cell surface antigens. In addition, the reaction rate should be in the appropriate range such that the desired click reaction is sufficiently slow in the diluted extracellular medium but fast enough to trigger cross-linking on the cell surface under increased effective concentrations.

LC-MS-based analysis of the reaction of glycine-conjugated AbCs (Table S1, Figure S1) revealed that the second-order reaction rates of click reactions with Tz- and BCN-linkers and MTz- and BCN-linkers were in the ranges of  $k = 10^2–10^5$  ( $M^{-1} s^{-1}$ ) and  $10^0–10^1$  ( $M^{-1} s^{-1}$ ), respectively (Figures 1b,c and S2). Next, we studied the click reactions of antibodies modified by the glycine-conjugated AbCs. Trastuzumab (anti-HER2 antibody) was labeled using AbCs ( $4.06 \pm 0.19$  AbC molecules per antibody; Figure S3), and the reaction between clickable pairs was monitored using SDS-PAGE. The results

Received: May 15, 2020

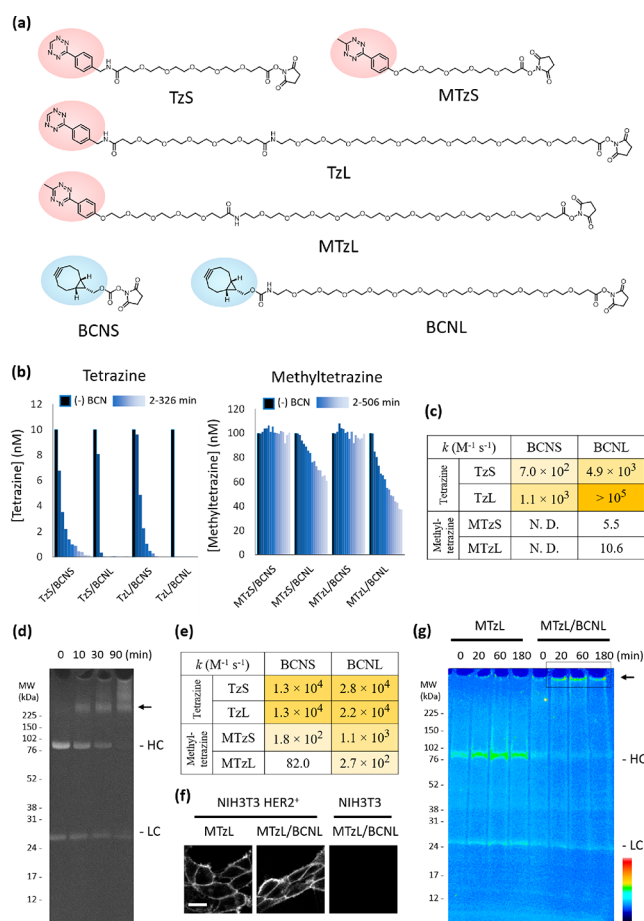


**Figure 1.** Synthesis and characterization of antibody clickers (AbCs). (a) Structures of AbCs. Tz = tetrazine, MTz = methyltetrazine, and BCN = bicyclononyne. (b) Monitoring of click reactions via pseudo-first-order kinetics of tetrazine consumption. The peaks were compared with one in the analysis without BCN (indicated with (–) BCN). (c) Calculated second-order rate constants of the click reactions in (b). Value  $\pm$  standard deviation (SD) ( $n = 3$ ). (d) Fluorescence image of the SDS-PAGE gel of trastuzumab labeled with MTzS and TAMRA (100 nM) mixed with trastuzumab labeled with BCNL (1000 nM) in PBS (pH 7.4). HC = heavy chain, LC = light chain. Protein bands with large molecular weights are indicated by a black arrow. Gel images for other click pairs are shown in Figure S4. (e) Calculated second-order rate constant of the reactions in (d). Value  $\pm$  SD ( $n = 3$ ). (f) Confocal fluorescence images of 3T3 HER2<sup>+</sup> and intact NIH3T3 cells incubated with Tra-MTzL with or without Tra-BCNL for 20 min. Antibodies were labeled with TAMRA, and total antibody concentration was 100 nM. Scale bar = 10  $\mu$ m. (g) Analysis of cell lysate by SDS-PAGE. Cells were incubated with Tra-MTzL with or without Tra-BCNL for 0–180 min. Antibodies were labeled with TAMRA, and total antibody concentration was 100 nM.

confirmed that they generated larger molecular weight species and aggregate-like structures (i.e., bands with no migration) in a time-dependent manner (Figure 1d). The labeling rate was in the order of  $k = 10^1$ – $10^4$  ( $M^{-1} s^{-1}$ ) in both Tz/BCN and MTz/BCN pairs (Figures 1e, S4, and S5). The discrepancy between small molecular and antibody click reactions might have stemmed from the modified antibody with basal interactions in the solution, allowing the non-ideal clickable pairs to exhibit cross-linking. As a representative example, trastuzumab labeled with MTzL/BCNL pairs exhibited a  $k = 2.7 \times 10^2$  ( $M^{-1} s^{-1}$ ); so, when the extracellular antibody concentrations were 100 nM, the calculated  $\tau_{1/2}$  (time for the

antibody to reach 50% of the initial concentration) would have been approximately 10 h. The labeling efficiency was not significantly affected in human serum (Figure S6).

We next tested whether the cross-linking reaction of AbC-labeled trastuzumab was facilitated after binding to the surface of HER2-overexpressing NIH3T3 cells (3T3 HER2<sup>+</sup>).<sup>9</sup> The cell surface was sufficiently labeled with the antibody after 20 min under both non-click (MTzL) and click (MTzL/BCNL) conditions (Figures 1f, S7, and S8). In the SDS-PAGE analysis of the cell lysate, the latter condition resulted in the major antibody population forming cross-linking products, even after 20 min (Figure 1g). The cross-linking products were observed only at low levels in the extracellular media during the same period (Figure S9), supporting our initial hypothesis that antibody cross-linking was facilitated on the cell surface.

Next, we examined whether the aggregation of antibodies on the cell surface altered their fates after target binding. We found that the antibodies were efficiently internalized after 1–3 h under click conditions (Figure 2a). This phenomenon was dependent on the linker length, and shorter linkers were relatively inefficient in forming the dot-like structures (Figure S10), presumably because the linkers were not long enough to connect with the antibodies when bound to the cell surface. At this point, aggregate formation in the extracellular medium compared with that on the cell surface contributed to the increased antibody uptake. To test this hypothesis, previously prepared clicked antibody products were added to the cells. As facilitated uptake was not observed under these conditions (Figure S11), antibodies forming aggregates after binding to the target made a major contribution to their increased cellular uptake.

Aggregate formation and facilitated uptake were more robustly observed when two antibodies that targeted different sites of HER2 were applied. The click reaction between trastuzumab and pertuzumab, which target domain IV and domain II of HER2, respectively, generated robust aggregates that were also efficiently taken up by cells (Figures 2b,c and S12). The efficiency of antibody uptake was studied by modifying the antibody with the pH-responsive fluorescent probe RhP-M<sup>13</sup> to selectively detect antibodies accumulated in the acidic intracellular environment (i.e., endosomal compartments; Figure 2d). Increased fluorescence was observed under click conditions (Figures S13–S15), confirming that an increased number of antibodies was taken up by cells due to the increased endocytosis.

Next, we tested whether this was a general effect using other cells and antibodies; HER2-overexpressing tumor cells NCI-N87 and SKBR3 were subjected to the facilitated endocytosis of trastuzumab under click conditions (Figures S16–S18). In addition, the facilitated endocytosis of the EGFR-targeting antibody panitumumab was observed in the EGFR-overexpressing tumor cells A431 (Figures S19 and S20).

The results indicated that the strategy described herein is generally applicable for increasing the uptake and accumulation of chemically modified antibodies for the better delivery of cargo, and is especially useful for the development of systems requiring efficient endosomal delivery of antibodies, such as antibody-based therapeutics<sup>4,5</sup> and molecular imaging.<sup>8</sup>

Besides facilitation of endocytosis, we found that cellular shape was modified upon the cross-linking of antibodies on the cell surface. In the system involving 3T3 HER2<sup>+</sup> and trastuzumab, notable rounding and clustering of the cells were observed, seemingly by the pulling cells toward each

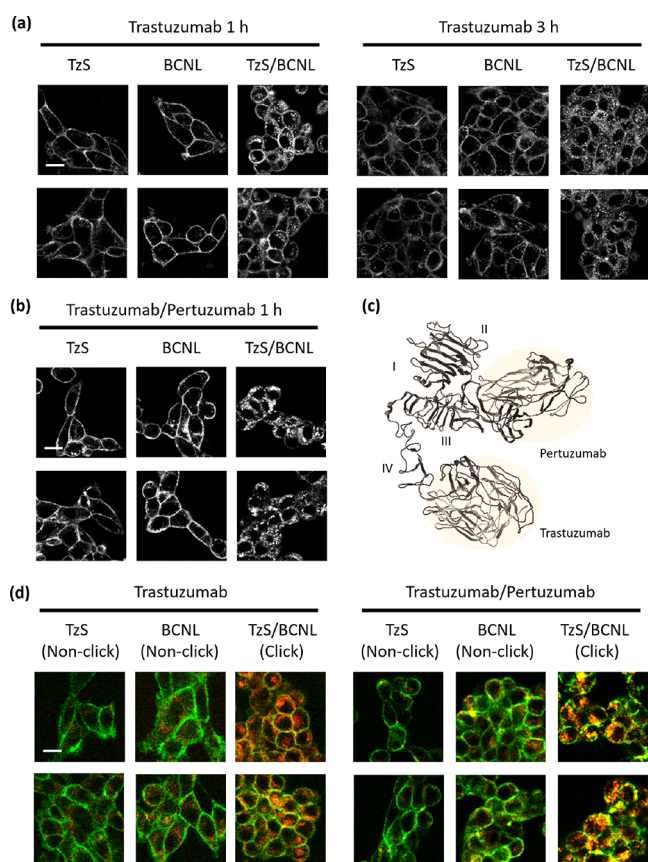


**Figure 2.** Cell surface click reactions facilitated the endocytosis of antibodies. (a) Confocal fluorescence images of 3T3 HER2<sup>+</sup> cells incubated with Tra-TzS, Tra-BCNL, or both. In all conditions, antibodies were labeled with TAMRA, and total antibody concentration was 100 nM. The results for other click pairs are shown in [Figure S10](#). Scale bar = 10  $\mu$ m. (b) Confocal fluorescence images of 3T3 HER2<sup>+</sup> cells incubated with Tra-TzS and pertuzumab labeled with TzS (Per-TzS; left), Tra-BCNL and Per-BCNL (center), and Tra-TzS and Per-BCNL (right). In all conditions, antibodies were labeled with TAMRA, and total antibody concentration was 100 nM. Scale bar = 10  $\mu$ m. (c) The binding model of trastuzumab and pertuzumab on the HER2 protein. The structure was derived from PDB ID 6OGE.<sup>14</sup> (d) Confocal fluorescence images of 3T3 HER2<sup>+</sup> cells indicated mixtures of Tra-TzS, Tra-BCNL, Per-TzS, and Per-BCNL. In all conditions, antibodies were labeled with Alexa Fluor 488 (green) and RhP-M (red). Total antibody concentration was 100 nM. Scale bar = 10  $\mu$ m.

other by intercellular click reactions ([Figures 3](#), [S21](#), and [S22](#), [Movie S1](#), and [Movie S2](#)). These effects were more robustly observed in the clickable pair of trastuzumab and pertuzumab ([Figure S23](#), [Movie S3](#)) but were not observed for the pre-clicked antibodies ([Figure S24](#)). Despite the risk that the overall phenomenon could damage the cells, the cells survived for 24 h, with no significant effects on cell viability ([Figures S22](#) and [S25](#)).

An interesting observation to note in the case of HER2-expressing SKBR3 cells was that an increased growth of cells was observed, rather than cell damage. In this, robust membrane blebbing and the formation of vesicle-like structures were observed ([Figure 4a](#), [Movie S4](#), and [Movie S5](#)), and cells seemed to show adherent and spreading phenotypes after 3 h ([Figure S26](#)). We speculated that these phenomena were due to the activation of intracellular growth signaling, and we

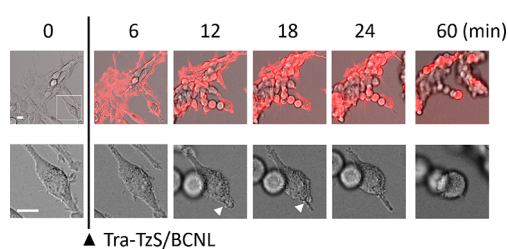


**Figure 3.** Cell surface click reaction affected the cellular shape. (Upper) Overlay of bright-field images and fluorescence images (red) of 3T3 HER2<sup>+</sup> cells after the addition of TAMRA-labeled Tra-TzS (50 nM) and Tra-BCNL (50 nM). The mixture of antibodies was added between 3 and 6 min (indicated by a black arrowhead). (Lower) Magnified version of the upper image (white rectangle). White arrowheads indicate the blebbing structures. Scale bar = 10  $\mu$ m. Further details are shown in [Movie S1](#).

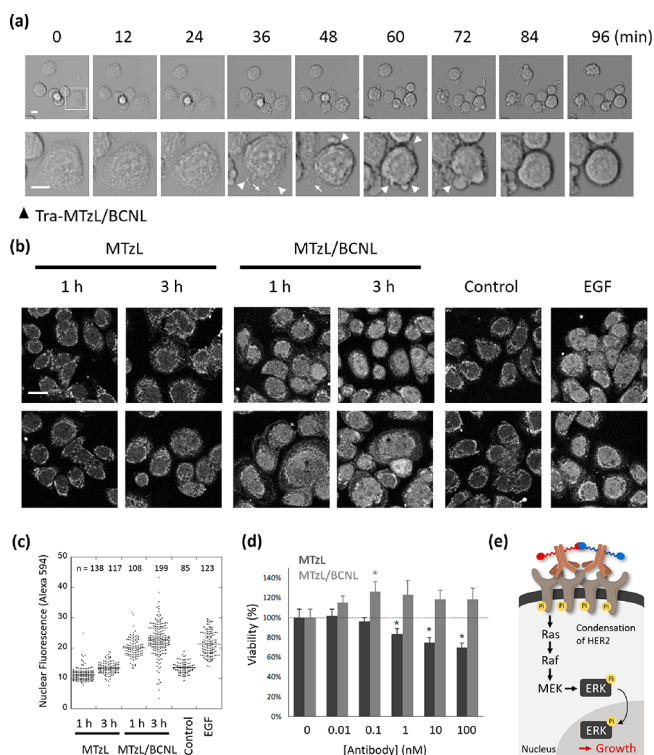


**Figure 4.** Cell surface click-reaction-modified intracellular signaling pathways of HER2-expressing tumor cells. (a) Bright-field images of SKBR3 cells after the addition of TAMRA-labeled Tra-MTzL (50 nM) and Tra-BCNL (50 nM). Arrowheads indicate the blebbing structures, and arrows indicate the vesicle-like structures. Scale bar = 10  $\mu$ m. Further details are shown in [Movie S4](#). (b) Result of immunofluorescence staining of phosphor-ERK after incubation of SKBR3 cells with Tra-MTzL with or without Tra-BCNL. Total antibody concentration was 100 nM. For the positive control of pERK signaling activation, cells were treated with EGF (100 ng/mL) for 1 h. Scale bar = 10  $\mu$ m. (c) Quantification of nuclear pERK signaling in (b). Numbers in the column indicate the cell numbers included in each analysis. (d) Viability of SKBR3 cells after treatment with Tra-MTzL with or without Tra-BCNL for 2 d. Error bars represent SD ( $n = 8$ ). \* $P < 0.05$  (Student's  $t$  test). (e) Schematic view of antibody clicking activating the intracellular growth signaling.

questioned whether the phosphorylation of ERK, a major signaling molecule downstream of HER2, involved in increased cellular growth, would be activated; immunostaining revealed that strong nuclear phospho-ERK signaling was observed after

antibody clicking (Figure 4b,c). After 2 d of treatment, trastuzumab without the click reaction reduced the cell numbers, presumably by the blockade of growth signals, but, under click conditions, the antibody treatment resulted in increased cell numbers in a dose-dependent manner (Figure 4d). Thus, with and without clicking, the antibody triggered completely different fates, growth promotion and inhibition, of the cells. We consider that aggregation of the antibodies induced the condensation of the targeted receptor on the cell surface and facilitated cross-phosphorylation (Figure 4e). As condensation of the receptors on cell surface was utilized to activate various types of receptors,<sup>15,16</sup> we believe that the methodology to trigger it using the external antibodies will serve as a unique synthetic biology tool to modify cellular fate in clinical and biological samples as desired.

In conclusion, we developed a novel methodology for modulating the physical properties of antibodies on cell surfaces by facilitating intramolecular cross-linking via increased effective concentrations. We discovered that the cross-linking could alter antibody behaviors by increasing the endocytosis rate and modulating the cellular signaling pathways. The generality of the methodology will allow for various future applications, such as increasing the effectiveness of antibodies in cargo delivery and as synthetic biology tools to modify intracellular signaling pathways of interest using rational design.

## ■ ASSOCIATED CONTENT

### SI Supporting Information

The Supporting Information is available free of charge at <https://pubs.acs.org/doi/10.1021/jacs.0c05331>.

Methods, detailed information on synthesis and characterization of compounds, and supplementary data, including Scheme S1, Table S1, and Figures S1–S26 (PDF)

Movie S1, bright-field images of 3T3 HER2+ cells after the addition of TAMRA-labeled Tra-TzS (50 nM) and Tra-BCNL (50 nM) (AVI)

Movie S2, bright-field images of 3T3 HER2+ cells after the addition of TAMRA-labeled Tra-TzS (100 nM) (AVI)

Movie S3, bright-field images of 3T3 HER2+ cells after the addition of TAMRA-labeled Tra-TzS (50 nM) and Per-BCNL (50 nM) (AVI)

Movie S4, bright-field images of SKBR3 cells after the addition of TAMRA-labeled Tra-TzS (50 nM) and Tra-BCNL (50 nM) (AVI)

Movie S5, bright-field images of SKBR3 cells after the addition of TAMRA-labeled Tra-TzS (100 nM) (AVI)

## ■ AUTHOR INFORMATION

### Corresponding Authors

**Toru Komatsu** – Graduate School of Pharmaceutical Sciences, The University of Tokyo, Tokyo 113-0033, Japan;  
orcid.org/0000-0002-9268-6964; Email: [tkomatsu@mol.fu-tokyo.ac.jp](mailto:tkomatsu@mol.fu-tokyo.ac.jp)

**Yasuteru Urano** – Graduate School of Pharmaceutical Sciences and Graduate School of Medicine, The University of Tokyo, Tokyo 113-0033, Japan; Core Research for Evolutional Science and Technology (CREST), Japan Agency for Medical Research and Development (AMED), Tokyo 100-0004, Japan;

orcid.org/0000-0002-1220-6327; Email: [uranokun@m.u-tokyo.ac.jp](mailto:uranokun@m.u-tokyo.ac.jp)

## Authors

**Etsu Kyo** – Graduate School of Pharmaceutical Sciences, The University of Tokyo, Tokyo 113-0033, Japan

**Haruki Ishii** – Graduate School of Pharmaceutical Sciences, The University of Tokyo, Tokyo 113-0033, Japan

**Kyoji Tsuchikama** – Texas Therapeutics Institute, The Brown Foundation Institute of Molecular Medicine, The University of Texas Health Science Center at Houston, Houston, Texas 77054, United States; orcid.org/0000-0002-2359-0408

**Aiko Yamaguchi** – Texas Therapeutics Institute, The Brown Foundation Institute of Molecular Medicine, The University of Texas Health Science Center at Houston, Houston, Texas 77054, United States

**Tasuku Ueno** – Graduate School of Pharmaceutical Sciences, The University of Tokyo, Tokyo 113-0033, Japan;

orcid.org/0000-0001-6657-8209

**Kenjiro Hanaoka** – Graduate School of Pharmaceutical Sciences, The University of Tokyo, Tokyo 113-0033, Japan;

orcid.org/0000-0003-0797-4038

Complete contact information is available at:

<https://pubs.acs.org/10.1021/jacs.0c05331>

## Notes

The authors declare no competing financial interest.

## ■ ACKNOWLEDGMENTS

Financial support for this study was provided by MEXT (24655147, 15H05371, 15K14937, 17K19477, 18H04538, 19H02846, and 20H04694 to T.K.), JST (PRESTO, PRESTO Network, and CREST to T.K.), AMED (CREST to Y.U.), and the DoD (W81XWH-18-1-0004 and W81XWH-19-1-0598 to K.T.). The project was also supported by JSPS Core-to-Core program (JPJSCCA20170007). T.K. was supported by The Naito Foundation, The Mochida Memorial Foundation for Medical and Pharmaceutical Research, and The Tokyo Biochemical Research Foundation.

## ■ REFERENCES

- (1) Rouge, L.; Chiang, N.; Steffek, M.; Kugel, C.; Croll, T. I.; Tam, C.; Estevez, A.; Arthur, C. P.; Koth, C. M.; Ciferri, C.; Kraft, E.; Payandeh, J.; Nakamura, G.; Koerber, J. T.; Rohou, A. Structure of CD20 in complex with the therapeutic monoclonal antibody rituximab. *Science* **2020**, *367* (6483), 1224–1230.
- (2) Kang, J. C.; Sun, W.; Khare, P.; Karimi, M.; Wang, X.; Shen, Y.; Ober, R. J.; Ward, E. S. Engineering a HER2-specific antibody-drug conjugate to increase lysosomal delivery and therapeutic efficacy. *Nat. Biotechnol.* **2019**, *37* (5), 523–526.
- (3) Li, J. Y.; Perry, S. R.; Muniz-Medina, V.; Wang, X.; Wetzel, L. K.; Rebelatto, M. C.; Masson Hinrichs, M. J.; Bezabeh, B. Z.; Fleming, R. L.; Dimasi, N.; Feng, H.; Toader, D.; Yuan, A. Q.; Xu, L.; Lin, J.; Gao, C.; Wu, H.; Dixit, R.; Osbourn, J. K.; Coats, S. R. A biparatopic HER2-targeting antibody-drug conjugate induces tumor regression in primary models refractory to or ineligible for HER2-targeted therapy. *Cancer Cell* **2019**, *35* (6), 948–949.
- (4) Alley, S. C.; Okeley, N. M.; Senter, P. D. Antibody-drug conjugates: targeted drug delivery for cancer. *Curr. Opin. Chem. Biol.* **2010**, *14* (4), 529–537.
- (5) Anami, Y.; Yamazaki, C. M.; Xiong, W.; Gui, X.; Zhang, N.; An, Z.; Tsuchikama, K. Glutamic acid-valine-citrulline linkers ensure stability and efficacy of antibody-drug conjugates in mice. *Nat. Commun.* **2018**, *9* (1), 2512.

(6) Mitsunaga, M.; Ogawa, M.; Kosaka, N.; Rosenblum, L. T.; Choyke, P. L.; Kobayashi, H. Cancer cell-selective in vivo near infrared photoimmunotherapy targeting specific membrane molecules. *Nat. Med.* **2011**, *17* (12), 1685–1691.

(7) Sato, K.; Ando, K.; Okuyama, S.; Moriguchi, S.; Ogura, T.; Totoki, S.; Hanaoka, H.; Nagaya, T.; Kokawa, R.; Takakura, H.; Nishimura, M.; Hasegawa, Y.; Choyke, P. L.; Ogawa, M.; Kobayashi, H. Photoinduced ligand release from a silicon phthalocyanine dye conjugated with monoclonal antibodies: a mechanism of cancer cell cytotoxicity after near-infrared photoimmunotherapy. *ACS Cent. Sci.* **2018**, *4* (11), 1559–1569.

(8) Mestel, R. Cancer: Imaging with antibodies. *Nature* **2017**, *543* (7647), 743–746.

(9) Urano, Y.; Asanuma, D.; Hama, Y.; Koyama, Y.; Barrett, T.; Kamiya, M.; Nagano, T.; Watanabe, T.; Hasegawa, A.; Choyke, P. L.; Kobayashi, H. Selective molecular imaging of viable cancer cells with pH-activatable fluorescence probes. *Nat. Med.* **2009**, *15* (1), 104–109.

(10) Oliveira, B. L.; Guo, Z.; Bernardes, G. J. L. Inverse electron demand Diels-Alder reactions in chemical biology. *Chem. Soc. Rev.* **2017**, *46* (16), 4895–4950.

(11) Tamura, T.; Hamachi, I. Chemistry for covalent modification of endogenous/native proteins: From test tubes to complex biological systems. *J. Am. Chem. Soc.* **2019**, *141* (7), 2782–2799.

(12) Sakamoto, S.; Hamachi, I. Recent Progress in Chemical Modification of Proteins. *Anal. Sci.* **2019**, *35* (1), 5–27.

(13) Watanabe, R.; Soga, N.; Fujita, D.; Tabata, K. V.; Yamauchi, L.; Hyeon Kim, S.; Asanuma, D.; Kamiya, M.; Urano, Y.; Suga, H.; Noji, H. Arrayed lipid bilayer chambers allow single-molecule analysis of membrane transporter activity. *Nat. Commun.* **2014**, *5*, 4519.

(14) Hao, Y.; Yu, X.; Bai, Y.; McBride, H. J.; Huang, X. Cryo-EM Structure of HER2-trastuzumab-pertuzumab complex. *PLoS One* **2019**, *14* (5), e0216095.

(15) Fegan, A.; White, B.; Carlson, J. C.; Wagner, C. R. Chemically controlled protein assembly: techniques and applications. *Chem. Rev.* **2010**, *110* (6), 3315–3336.

(16) Ueki, R.; Uchida, S.; Kanda, N.; Yamada, N.; Ueki, A.; Akiyama, M.; Toh, K.; Cabral, H.; Sando, S. A chemically unmodified agonistic DNA with growth factor functionality for in vivo therapeutic application. *Sci. Adv.* **2020**, *6* (14), eaay2801.